

YZ Phoenicis: Photometric Study of a W UMa Binary Near the Short-period Limit

RONALD G. SAMEC^{1,2}

Department of Physics and Astronomy, Millikin University, Decatur, Illinois 62522
 Electronic mail: rsamec@mail.millikin.edu

DIRK TERRELL³

Department of Astronomy, University of Florida, Gainesville, Florida 32609
 Electronic mail: terrell@algol.iras.ucalgary.ca

Received 1994 July 14; accepted 1995 February 13

ABSTRACT. An analysis of *BVRI* photometry of the high galactic southern latitude W UMa variable, YZ Phe, is reported. The photometry was done in November 1989 at Cerro Tololo Inter-American Observatory. Four new precision epochs of minimum light were determined and improved linear ephemerides were computed from all available epochs. The period study indicates that its period has probably remained constant at $0^d.23472$ over the 30-yr interval it has been observed. A large O'Connell effect is present in the light curves with the maximum following Min II ~ 0.1 mag brighter in B than the maximum following Min I. A brief ~ 15 -min interval of constant light is discernible in the primary eclipse, indicating that the more-massive component is the cooler. A four-color simultaneous computation including a second-order reflection effect strongly favored the presence of a large 54° radius superluminous region instead of the usual dark spot on the cooler component with a temperature factor of only 1.03. Further, we find that the system consists of two early K spectral-type dwarfs in marginal contact with $\sim 2\%$ fill out, and a mass ratio of ~ 0.40 .

1. INTRODUCTION

Our investigations (Samec et al. 1993a; Samec, Su, and DeWitt 1993b; Samec and Hube 1991; Samec 1990, etc.) of solar-type eclipsing binaries have usually been confined to those having the shortest-known orbital periods or very-short period, VSP systems. We have defined VSP systems as those having periods, $P \leq 0^d.30$. Many of them have been found to be in a state of high activity and rapid orbital evolution. With orbital velocities of several hundreds of km/s, and convective envelopes, the components possess strong dynamo-driven magnetic fields. This results in high chromospheric activity, stellar winds, and rapid mass and angular momentum loss (Soderblom et al. 1993; Eggleton 1992). Magnetic activity reaches such a level that their surfaces are likely saturated, e.g., there is "a total filling in of the stellar surfaces by magnetic structures" (Soderblom et al. 1993; Rucinski 1993). Not only do VSP systems delineate the highest levels of emission lines such as Mg II (Rucinski 1993), but recently, a constant emission of hard X rays in the 2–10 keV was detected from VW Cep (Tsuru et al. 1992). Here, we continue this study with the photometric investigation of one of the shortest-period systems known, YZ Phoenicis.

The high galactic southern latitude W UMa variable, YZ Phe [S 7172, $\alpha(2000) = 01^h 42^m 23^s$, $\delta(2000) = -45^\circ 56' 56''$; galactic latitude, $\beta = +68^\circ 64'$], was discovered by Hoffmeister (1963) and classified as an Algol type. A finding chart is

included in his paper on page 33. Gessner and Meinunger (1975), hereafter referred to as GM, gave seven times of minimum light from which they determined a provisional period of $0^d.3052$. These timings are listed in our Table 3. Fourteen-years later, Jones (1989) published *UBVRI* observations covering the phases from $\sim 0^p.6$ to $0^p.2$ (Jones had arbitrarily defined his minimum at $0^p.5$ which is really a primary eclipse). He determined standard magnitudes for Min I ($0^p.25$), and the maximum at $0^p.75$, or Max II. These values are given in Table 2. He also determined $U - B = 0.61(3)$ at Min I, and a precision timing of minimum light given in our Table 3. He states that the period given by GM is most likely a "1 day alias" of the true period at that epoch, $\sim 0^d.234$. His *U* light curve is quite noisy which might be indicative of hot photometric flaring episodes. Kilkenny and Marang (1990), hereafter referred to as KM, published an IBVS report on *UBVR_cI_c* observations showing a complete *V* light curve with a very large O'Connell effect, the magnitude difference between Max II and Max I being ~ -0.1 . Their nine timings of minimum light are listed in Table 3. It is interesting that their observations were made before, during, and after our observing run. Using a phase-dispersion minimization technique, they determined an orbital period of $0^d.234726(2)$. KM decided not to link the earlier GM timings (as is done in this paper) with their own due to the large gap in the observations. Using Hill's LIGHT2, Holmgren (1991) calculated a simultaneous *BVRI* solution to the observations of KM obtaining these preliminary values: $r_1 = 0.422$, $r_2 = 0.344$, $T_1 = T_2 = 5200$ K, $q = m_2/m_1 = 0.621$, $i = 79.8(1)$ and fill out, $f = 0.33$, where subscript "1" refers to the more massive primary component and "2" to the secondary component. Here, we define the fill-out ratio as

¹Visiting astronomer, Cerro Tololo Inter-American Observatory, National Optical Astronomical Observatories, which are operated by the Association of Universities for Research in Astronomy, Inc. under contract with the National Science Foundation.

²This research was partially supported by a grant from NASA administered by the American Astronomical Society.

³Present address: Department of Physics and Astronomy, University of Calgary, 2500 University Dr., NW, Calgary, AB, Canada.

$$f = \frac{\Omega_1 - \Omega_{\text{ph}}}{\Omega_1 - \Omega_2},$$

where the potentials Ω_1 and Ω_2 define the inner and outer critical surfaces in Roche Geometry and Ω_{ph} is the photometrically determined value. He gave no information on how he handled the large asymmetry, which is a crucial detail in modeling this system. Among the nondegenerate binaries with well-confirmed periods, YZ Phe has the third-shortest orbital period, slightly longer than that of CC Com, $P=0^d2207$, and V523 Cas, $P=0^d2337$. These binaries define the short-period limit for nondegenerate dwarfs (Rucinski 1992). One reported $0^d2038504$ period binary (Hoffleit 1963), V1961 Sgr has been recently observed by RS and found to be of W-UMa type (rather than Algol) with a period near 13 hr! Five other eclipsing variables are purported to have periods between 0^d22 and 0^d24 . These include four variables in Ophiuchus, V954, V1022, V1892, and V2060 Oph, and the well-known RW Com. However, recent CCD observations of V954 Oph by RS showed no variation to within scatter bands of 0.01 mag over a 90-min observational interval. It is of interest that no other systems have confirmed periods less than 0^d22 except in the case of a recent account of visual observations by Dedoch (1991) of the variable NSV 5598 which was discovered by Archer (1959). This object is said to be a W UMa variable with a period of $0^d115!$ We suspect that it is a Delta Scuti variable.

2. OBSERVATIONS

The observations of YZ Phe were made on 1989 November 2–8, inclusive, at Cerro Tololo Inter-American Observatory, Chile, South America. The Yale 1 m $f/10.5$ Ritchey–Chrétien telescope was used with the dry-ice-cooled Hamamatsu R943-02 Ga-As PMT, cold box 71, with a 19.5-in.-diameter focal plane diaphragm. The automated single channel aperture photometer system was used. The procedures, involving standard differential photometry (Henden and Kaitchuck 1990; Hardie 1962), were the same as those detailed previously (Samec, Charlesworth, and DeWitt 1991). The integration times were varied somewhat so that photon noise would not keep the photometric precision from being as good as 1%. Two nearby stars, within $10'$, and both northward of the variable, a twelfth magnitude star at $\alpha(2000)=01^h 42^m 29^s$, $\delta(2000)=-45^\circ 52' 35''$, and an eleventh magnitude star at $\alpha(2000)=01^h 42^m 21^s$, $\delta(2000)=-45^\circ 53' 54''$ were used as comparison and check stars. The comparison star matched well the color of the variable with $\Delta(B-V) \sim -0.07$ and $\Delta(R-I) \sim 0.03$. Measurements of the check star indicated that the light of the comparison star stayed constant throughout the observing interval. Differential extinction corrections were found to be on the order of $\sim 0^m001$ and were not applied to the observations. The individual observations, 477 with the B filter, 473 with the V filter, 526 with the R filter, and 529 with the I filter are given in Table 1 as Heliocentric (or Barycentric) Julian Date (HJD) versus magnitude difference Delta Mag. The later are given as variable minus comparison star.

3. STANDARD MAGNITUDES

The magnitudes were transformed to the Johnson–Cousins system (Landolt 1983; Bessell 1976, 1979). Five to seven standard star measurements of Landolt (1983) $UBVR_cI_c$ photometric standards were taken every evening. In two recent papers (Samec et al. 1993a; Samec, Su, and DeWitt 1993b) we carelessly designated the Landolt selected area stars 102 58, 103 462, 103 302, 103 526, 103 302, 103 526, 105 66, 105 205, 105 405, 105 448, 105 663, 106 1024, 107 347, 107 595, 108 475, 108 551, 108 702, 108 1332, 111 2009, 111 2512, 111 2522, 111 717, 111 775, 111 2522, 121 960, 148 817, 149 382 as HD stars. We apologize to the Strasbourg Astronomical Data Center for the confusion this has caused in the SIMBAD data base.

Primary extinction coefficients, which were used in the calculation of the transformations (Hardie 1962), were determined from nightly comparison star measurements. The coefficients, when applied to the standard stars, reproduced their standard magnitudes with probable errors of ± 2 to ± 11 mmag. Our standard magnitude determinations are given in Table 2 along with those by Jones (1989). The magnitudes of the comparison and check star are mean values of determinations from the three most stable nights. Each variable star standard magnitude is the mean calculated from 4 to 8 determinations occurring within $\sim \pm 0^p02$ of the phase in question. In Table 2 and throughout this paper, values are accompanied by their probable errors shown in parentheses. Both the high galactic latitude, and the $(B-V)$, $(R-I)$, and $(V-I)$ color indices indicate that the interstellar reddening is negligible. At phase 0^p0 , the primary (occluding) component has color indices (Popper 1980; Bessell 1979) which indicate it has a spectral type of K3(V). The indices at phase 0^p25 were used to determine that the secondary component is of spectral-type K2(V). The comparison star is of spectral-type K3–4(V) and the check star is G5(V). All color indices were consistent with these results except for the $U-B$ value for the variable given by Jones (1989) which suggests that the primary component is of a slightly hotter K1(V) spectral type. In the period–color plane for W UMa variables, updated by Rucinski (1992), YZ Phe falls near the left, short-period edge ($\log P = \pm 0.629$), and on the upper or hotter edge. Thus, it appears that YZ Phe is somewhat blue, and thus, rather massive for its period.

4. PERIOD ANALYSIS

Four epochs of minimum light were determined from $BVRI$ observations made during one primary and three secondary eclipses. The timings were determined graphically by the bisection of chords technique (Henden and Kaitchuck 1990). This technique was used since most of the nightly eclipse curves were not evenly covered. Our epochs of minimum light are given in Table 3 as means of times from the four bandpasses along with their probable errors. All other epochs of minimum light found in the literature are also included in Table 3. These data span 30 years of observations or about 47,000 orbital revolutions. However, a large 37,000 cycle gap follows the initial timings of GM. Taking only the timings of GM, we recalculated linear least-squares eph-

TABLE 1
Observations of YZ Phoenixis

B OBSERVATIONS									
JD HEL. 2447830+	DELTA B MAG	JD HEL. 2447830+	DELTA B MAG	JD HEL. 2447830+	DELTA B MAG	JD HEL. 2447830+	DELTA B MAG	JD HEL. 2447830+	DELTA B MAG
2.6346	0.3443	3.7178	0.1475	4.7771	-0.0134	6.7011	-0.2728	6.8199	-0.1785
2.6352	0.3590	3.7186	0.0956	4.7781	-0.0195	6.7018	-0.2681	6.8206	-0.1683
2.6359	0.3611	3.7196	0.0777	4.7788	-0.0294	6.7028	-0.2672	6.8220	-0.1626
2.6370	0.3806	3.7204	0.0645	4.7795	-0.0726	6.7035	-0.2699	6.8227	-0.1823
2.6378	0.3986	3.7211	0.0454	4.7827	-0.1020	6.7042	-0.2602	6.8234	-0.1741
2.6386	0.4512	3.7223	0.0276	4.7834	-0.1176	6.7052	-0.2561	6.8279	-0.1325
2.6425	0.4134	3.7230	-0.0016	4.7841	-0.1113	6.7059	-0.2555	6.8288	-0.1337
2.6432	0.4093	3.7238	0.0081	4.7851	-0.1196	6.7066	-0.2470	6.8295	-0.1379
2.6440	0.3982	3.7248	-0.0218	4.7858	-0.1299	6.7076	-0.2469	6.8302	-0.1336
2.6453	0.3885	3.7255	-0.0503	4.7865	-0.1388	6.7083	-0.2390	6.8311	-0.1208
2.6460	0.3923	3.7263	-0.0339	4.7875	-0.1239	6.7090	-0.2404	6.8318	-0.1036
2.6468	0.3739	3.7300	-0.0857	4.7882	-0.1561	6.7100	-0.2348	6.8325	-0.0995
2.6480	0.3433	3.7311	-0.0681	4.7888	-0.1673	6.7107	-0.2272	6.8357	-0.0882
2.6488	0.3239	3.7319	-0.0709	4.7898	-0.1720	6.7113	-0.2371	6.8364	-0.0797
2.6495	0.2985	3.7326	-0.0952	4.7905	-0.1806	6.7155	-0.1952	6.8370	-0.0803
2.6538	0.2246	3.7337	-0.1105	4.7912	-0.1692	6.7162	-0.1829	6.8380	-0.0588
2.6545	0.1972	3.7345	-0.0919	4.7923	-0.1918	6.7169	-0.1842	6.8387	-0.0468
2.6553	0.1790	3.7352	-0.0932	4.7930	-0.2071	6.7179	-0.1914	6.8394	-0.0321
2.6565	0.1410	3.7467	-0.1479	4.7937	-0.2165	6.7186	-0.1556	6.8403	-0.0440
2.6572	0.1046	3.7474	-0.1756	4.7970	-0.2316	6.7193	-0.1569	6.8410	-0.0334
2.6580	0.1099	3.7482	-0.1658	4.7977	-0.2256	6.7202	-0.1433	6.8417	-0.0143
2.6591	0.0941	3.7493	-0.1727	4.7984	-0.2252	6.7209	-0.1481	6.8428	-0.0147
2.6598	0.0590	3.7500	-0.1433	4.7994	-0.2573	6.7216	-0.1320	6.8434	-0.0089
2.6606	0.0815	3.7508	-0.1684	4.8001	-0.2515	6.7225	-0.1201	6.8441	0.0117
2.6641	-0.0322	3.7518	-0.1876	4.8008	-0.2376	6.7232	-0.1041	6.8451	0.0271
2.6649	-0.0313	3.7526	-0.1754	4.8041	-0.2506	6.7239	-0.0959	6.8458	0.0419
2.6657	-0.0600	3.7534	-0.1732	4.8048	-0.2584	6.7429	0.4186	6.8465	0.0756
2.6667	-0.0603	3.7549	-0.1767	4.8055	-0.2334	6.7436	0.4464	6.8981	-0.1708
2.6676	-0.0784	3.7557	-0.1851	4.8067	-0.2560	6.7443	0.4529	6.8988	-0.1621
2.6683	-0.1104	3.7565	-0.2010	4.8074	-0.2613	6.7452	0.4330	6.8995	-0.1877
2.6694	-0.0863	3.7601	-0.1907	4.8081	-0.2557	6.7459	0.4640	6.8701	-0.1969
2.6701	-0.1057	3.7608	-0.2018	4.8091	-0.2632	6.7466	0.4645	6.8708	-0.1722
2.6709	-0.1179	3.7616	-0.1914	4.8098	-0.2710	6.7476	0.4566	6.8702	-0.1752
2.6719	-0.1218	3.8058	0.2888	4.8105	-0.2595	6.7483	0.4482	6.8706	-0.1440
2.6727	-0.1363	3.8066	0.2852	4.8114	-0.2667	6.7489	0.4741	6.8708	-0.1406
2.6734	-0.1360	3.8073	0.2698	4.8121	-0.2707	6.7499	0.4886	6.8705	-0.1392
2.6772	-0.1773	3.8086	0.3229	4.8128	-0.2774	6.7506	0.4726	6.8707	-0.1387
2.6780	-0.1815	3.8094	0.3488	4.8160	-0.2713	6.7513	0.4756	6.8709	-0.1237
2.6787	-0.1808	3.8101	0.3665	4.8167	-0.2663	6.7522	0.4884	6.8710	-0.1090
2.6799	-0.1806	3.8114	0.3827	4.8174	-0.2620	6.7529	0.4776	6.8713	-0.0784
2.6807	-0.2098	3.8121	0.3842	4.8184	-0.2760	6.7536	0.4827	6.8714	-0.0647
2.6814	-0.1898	3.8129	0.4081	4.8191	-0.2889	6.7546	0.4478	6.8715	-0.0649
2.6856	-0.2176	3.8140	0.3787	4.8198	-0.2537	6.7553	0.4538	6.8716	-0.0435
2.6864	-0.2474	3.8147	0.4281	4.8208	-0.2752	6.7560	0.4606	6.8716	-0.0579
2.6872	-0.2539	3.8155	0.4349	4.8215	-0.2700	6.7591	0.4125	6.8715	-0.0386
2.6883	-0.2511	3.8191	0.4149	4.8222	-0.2426	6.7598	0.3735	6.8721	-0.0441
2.6891	-0.2479	3.8200	0.4059	4.8232	-0.2718	6.7605	0.3446	6.8721	-0.0088
2.6899	-0.2661	3.8208	0.3782	4.8239	-0.2767	6.7614	0.3144	6.8722	-0.0194
2.6910	-0.2572	3.8221	0.3408	4.8245	-0.2816	6.7623	0.2895	6.8723	0.0183
2.6918	-0.2700	3.8230	0.3471	4.8281	-0.2718	6.7632	0.2678	6.8724	0.0362
2.6925	-0.2654	3.8238	0.3050	4.8288	-0.2682	6.7651	0.2126	6.8724	0.0345
2.6935	-0.2783	3.8252	0.2771	4.8294	-0.2547	6.7660	0.1823	6.8725	0.1203
2.6943	-0.2853	3.8259	0.2628	4.8304	-0.2717	6.7667	0.1577	6.8729	0.1467
2.6951	-0.3126	3.8267	0.2706	4.8311	-0.2502	6.7674	0.1579	6.8729	0.1496
2.6961	-0.2900	3.8281	0.2273	4.8318	-0.2390	6.7685	0.1473	6.8730	0.1857
2.6969	-0.3036	3.8289	0.2006	4.8328	-0.2544	6.7692	0.1128	6.8731	0.2049

TABLE 1
(Continued)

B OBSERVATIONS (Continued)									
JD HEL. 2447830+	DELTA B MAG	JD HEL. 2447830+	DELTA B MAG	JD HEL. 2447830+	DELTA B MAG	JD HEL. 2447830+	DELTA B MAG	JD HEL. 2447830+	DELTA B MAG
2.6976	-0.3027	3.8296	0.1779	4.8335	-0.2278	6.7699	0.0839	8.7323	0.2286
2.7080	-0.2859	3.8349	0.0678	4.8342	-0.2297	6.7734	0.0334	8.7358	0.3079
2.7088	-0.2595	3.8357	0.0499	4.8352	-0.2311	6.7857	-0.1184	8.7365	0.3247
2.7095	-0.2332	3.8364	0.0381	4.8359	-0.2278	6.7861	-0.1055	8.7372	0.3570
2.7151	-0.2476	3.8375	0.0262	4.8366	-0.2117	6.7865	-0.1199	8.7381	0.3589
2.7167	-0.2358	3.8382	0.0023	4.8404	-0.1913	6.7873	-0.1165	8.7388	0.3863
2.7178	-0.2301	3.8390	-0.0186	4.8411	-0.2177	6.7877	-0.1323	8.7395	0.3977
2.7186	-0.2348	3.8401	-0.0645	4.8429	-0.1569	6.7881	-0.1222	8.7405	0.4166
2.7194	-0.2097	3.8409	-0.0547	4.8435	-0.1691	6.7888	-0.1239	8.7411	0.3975
2.7207	-0.2037	3.8416	-0.0638	4.8446	-0.1239	6.7892	-0.1373	8.7418	0.4053
2.7215	-0.2259	3.8428	-0.0619	4.8453	-0.1194	6.7896	-0.1549	8.7430	0.4424
2.7222	-0.1989	3.8436	-0.0948	4.8460	-0.0975	6.7903	-0.1270	8.7437	0.4259
2.7234	-0.1818	3.8444	-0.1080	5.8203	0.4160	6.7907	-0.1451	8.7483	0.4209
2.7242	-0.2057	4.7293	-0.0355	5.8211	0.4011	6.7911	-0.1470	8.7490	0.4104
2.7249	-0.1917	4.7302	-0.0125	5.8219	0.3719	6.7937	-0.1432	8.7499	0.3899
2.8193	-0.1713	4.7310	-0.0013	5.8231	0.3259	6.7944	-0.1377	8.7506	0.3896
2.8200	-0.1862	4.7321	0.0075	5.8239	0.3062	6.7951	-0.1482	8.7513	0.3970
2.8208	-0.2027	4.7328	0.0152	5.8247	0.2761	6.7970	-0.1612	8.7525	0.3105
2.8219	-0.2069	4.7335	0.0157	5.8259	0.2672	6.7980	-0.1597	8.7532	0.3214
2.8227	-0.1968	4.7359	0.0824	5.8267	0.2350	6.7987	-0.1645	8.7539	0.3092
2.8234	-0.1592	4.7369	0.0926	5.8275	0.2023	6.7994	-0.1670	8.7853	-0.2236
2.8250	-0.1957	4.7376	0.1008	5.8287	0.1638	6.8026	-0.1923	8.7860	-0.2287
2.8257	-0.2066	4.7383	0.1183	5.8295	0.1389	6.8033	-0.1891	8.7869	-0.2380
2.8265	-0.1890	4.7639	0.2798	5.8303	0.1046	6.8040	-0.1914	8.7876	-0.2343
2.8277	-0.1942	4.7646	0.2727	5.8344	0.0505	6.8050	-0.1895	8.7883	-0.2444
2.8284	-0.1655	4.7653	0.2433	5.8351	0.0039	6.8057	-0.1811	8.7893	-0.2699
2.8292	-0.1723	4.7663	0.2198	5.8357	0.0286	6.8064	-0.2001	8.7900	-0.2686
2.8345	-0.1550	4.7670	0.1952	5.8367	-0.0247	6.8073	-0.1881	8.8407	-0.0414
2.8353	-0.1221	4.7676	0.2071	5.8378	-0.0330	6.8080	-0.1781	8.8419	-0.0234
2.8360	-0.1392	4.7687	0.1623	5.8384	-0.0215	6.8087	-0.1919	8.8426	-0.0056
2.8371	-0.1298	4.7694	0.1399	5.8395	-0.0173	6.8098	-0.1934	8.8432	0.0049
2.8379	-0.1147	4.7701	0.1378	5.8402	-0.0248	6.8105	-0.1994	8.8444	0.0536
2.8386	-0.0860	4.7710	0.1124	5.8409	-0.0447	6.8112	-0.1751	8.8451	0.0845
2.8397	-0.1201	4.7717	0.0981	5.8447	-0.0836	6.8143	-0.1950	8.8458	0.1294
2.8405	-0.1018	4.7724	0.0714	5.8454	-0.1014	6.8150	-0.1839	8.8467	0.1251
2.8412	-0.0746	4.7734	0.0724	5.8461	-0.0987	6.8157	-0.1938	8.8474	0.1567
2.8423	-0.0928	4.7741	0.0527	5.8471	-0.0996	6.8167	-0.1868	8.8481	0.1898
2.8431	-0.1009	4.7748	0.0163	5.8477	-0.1007	6.8174	-0.1837		
2.8438	-0.0758	4.7758	-0.0078	5.8484	-0.1011	6.8181	-0.1910		
3.7171	0.1260	4.7765	0.0054	6.7004	-0.2950	6.8192	-0.1912		

TABLE 1
(Continued)

V OBSERVATIONS									
JD HEL. 2447830+	DELTA B MAG	JD HEL. 2447830+	DELTA B MAG	JD HEL. 2447830+	DELTA B MAG	JD HEL. 2447830+	DELTA B MAG	JD HEL. 2447830+	DELTA B MAG
2.6344	0.3715	3.7176	0.1842	4.7762	0.0642	5.8468	-0.0373	6.8172	-0.0965
2.6350	0.4015	3.7184	0.1842	4.7769	0.0620	5.8475	-0.0481	6.8179	-0.1201
2.6357	0.4067	3.7194	0.1505	4.7779	0.0365	5.8482	-0.0240	6.8190	-0.1016
2.6369	0.4252	3.7202	0.1199	4.7786	0.0095	6.7009	-0.1647	6.8197	-0.0996
2.6376	0.4442	3.7209	0.1326	4.7793	0.0089	6.7016	-0.1627	6.8204	-0.1125
2.6384	0.4603	3.7221	0.0936	4.7825	-0.0151	6.7026	-0.1653	6.8218	-0.1067
2.6423	0.4566	3.7228	0.0975	4.7832	-0.0210	6.7033	-0.1618	6.8225	-0.1063
2.6430	0.4743	3.7236	0.0778	4.7839	-0.0536	6.7040	-0.1625	6.8232	-0.0846
2.6438	0.4549	3.7246	0.0508	4.7849	-0.0572	6.7050	-0.1752	6.8293	-0.0602
2.6450	0.4544	3.7253	0.0554	4.7856	-0.0559	6.7057	-0.1653	6.8300	-0.0634
2.6458	0.4399	3.7261	0.0423	4.7863	-0.0724	6.7063	-0.1740	6.8309	-0.0599
2.6466	0.4543	3.7298	0.0095	4.7873	-0.0954	6.7074	-0.1514	6.8316	-0.0388
2.6478	0.4225	3.7309	0.0005	4.7880	-0.0799	6.7081	-0.1486	6.8323	-0.0348
2.6486	0.3982	3.7317	-0.0048	4.7886	-0.0871	6.7088	-0.1551	6.8355	-0.0137
2.6493	0.3740	3.7324	-0.0108	4.7896	-0.1002	6.7098	-0.1444	6.8362	-0.0013
2.6536	0.2850	3.7335	-0.0167	4.7903	-0.0928	6.7105	-0.1421	6.8368	0.0063
2.6543	0.2479	3.7343	-0.0311	4.7910	-0.1010	6.7111	-0.1312	6.8378	-0.0009
2.6551	0.2480	3.7350	-0.0341	4.7921	-0.1293	6.7153	-0.0961	6.8384	0.0230
2.6563	0.2316	3.7465	-0.0888	4.7928	-0.1231	6.7160	-0.1060	6.8391	0.0284
2.6570	0.2092	3.7472	-0.0870	4.7935	-0.1124	6.7167	-0.0914	6.8401	0.0263
2.6578	0.2012	3.7480	-0.0989	4.7968	-0.1432	6.7177	-0.0901	6.8408	0.0382
2.6589	0.1534	3.7491	-0.1145	4.7975	-0.1746	6.7184	-0.0823	6.8415	0.0342
2.6596	0.1483	3.7498	-0.1062	4.7982	-0.1622	6.7191	-0.0725	6.8425	0.0382
2.6604	0.1429	3.7506	-0.1009	4.7992	-0.1620	6.7200	-0.0614	6.8432	0.0674
2.6639	0.0744	3.7516	-0.1039	4.7999	-0.1667	6.7207	-0.0723	6.8439	0.0684
2.6647	0.0614	3.7524	-0.0974	4.8006	-0.1543	6.7214	-0.0418	6.8449	0.0952
2.6655	0.0353	3.7532	-0.1045	4.8039	-0.1747	6.7223	-0.0353	6.8456	0.0930
2.6665	0.0144	3.7547	-0.1112	4.8046	-0.1741	6.7230	-0.0289	6.8463	0.1086
2.6673	0.0160	3.7555	-0.1075	4.8053	-0.1680	6.7237	-0.0171	6.8463	0.1087
2.6681	-0.0101	3.7563	-0.1004	4.8065	-0.1777	6.7427	0.4553	6.8463	0.1087
2.6692	-0.0213	3.7599	-0.0967	4.8072	-0.1671	6.7434	0.4604	6.8979	-0.1206
2.6699	-0.0380	3.7606	-0.1095	4.8079	-0.1806	6.7441	0.4897	6.8986	-0.0671
2.6707	-0.0438	3.7614	-0.0937	4.8088	-0.1877	6.7450	0.4985	6.8993	-0.1150
2.6717	-0.0407	3.8056	0.2995	4.8095	-0.1754	6.7457	0.5304	8.7009	-0.1097
2.6725	-0.0587	3.8064	0.3270	4.8102	-0.1957	6.7464	0.5021	8.7015	-0.0916
2.6732	-0.0684	3.8071	0.3339	4.8112	-0.1742	6.7474	0.5026	8.7022	-0.1015
2.6770	-0.0961	3.8084	0.3751	4.8119	-0.1907	6.7480	0.5317	8.7059	-0.0641
2.6778	-0.0909	3.8092	0.3820	4.8126	-0.2033	6.7487	0.5148	8.7066	-0.0537
2.6785	-0.1067	3.8099	0.4085	4.8158	-0.1915	6.7497	0.5260	8.7073	-0.0624
2.6797	-0.0968	3.8112	0.4245	4.8165	-0.1786	6.7504	0.5369	8.7085	-0.0449
2.6805	-0.1201	3.8119	0.4490	4.8172	-0.1797	6.7511	0.5188	8.7092	-0.0496
2.6812	-0.1169	3.8127	0.4596	4.8182	-0.1932	6.7520	0.5349	8.7098	-0.0574
2.6854	-0.1628	3.8138	0.4522	4.8189	-0.1638	6.7527	0.5161	8.7135	-0.0424
2.6862	-0.1641	3.8145	0.4397	4.8196	-0.1828	6.7534	0.5417	8.7142	-0.0268
2.6870	-0.1580	3.8153	0.4615	4.8206	-0.1865	6.7544	0.5330	8.7149	-0.0172
2.6882	-0.1784	3.8189	0.4512	4.8213	-0.1766	6.7551	0.4998	8.7159	0.0128
2.6889	-0.1787	3.8198	0.4426	4.8220	-0.1600	6.7558	0.5118	8.7166	0.0153
2.6897	-0.2030	3.8206	0.4403	4.8229	-0.1519	6.7596	0.4317	8.7173	0.0241
2.6908	-0.1789	3.8219	0.3961	4.8236	-0.1719	6.7603	0.4140	8.7208	0.0595
2.6916	-0.1781	3.8227	0.3743	4.8243	-0.1784	6.7612	0.4090	8.7215	0.0628
2.6923	-0.1759	3.8236	0.3617	4.8278	-0.1462	6.7619	0.3850	8.7221	0.0768
2.6933	-0.1820	3.8250	0.3521	4.8285	-0.1558	6.7629	0.3684	8.7231	0.0866
2.6941	-0.1944	3.8257	0.3280	4.8292	-0.1683	6.7649	0.2955	8.7238	0.1036
2.6949	-0.1934	3.8265	0.2912	4.8302	-0.1419	6.7658	0.2988	8.7245	0.1306

TABLE 1
(Continued)

V OBSERVATIONS (Continued)									
JD HEL. 2447830+	DELTA V MAG	JD HEL. 2447830+	DELTA V MAG	JD HEL. 2447830+	DELTA V MAG	JD HEL. 2447830+	DELTA V MAG	JD HEL. 2447830+	DELTA V MAG
2.6959	-0.1954	3.8279	0.2645	4.8309	-0.1542	6.7665	0.2703	8.7283	0.1699
2.6967	-0.1997	3.8287	0.2671	4.8316	-0.1407	6.7672	0.2692	8.7290	0.1927
2.6974	-0.2009	3.8294	0.2344	4.8326	-0.1301	6.7682	0.2262	8.7297	0.2101
2.7078	-0.1928	3.8347	0.1252	4.8333	-0.1534	6.7690	0.2071	8.7307	0.2212
2.7086	-0.1638	3.8355	0.1083	4.8340	-0.1408	6.7697	0.1928	8.7314	0.2516
2.7093	-0.1702	3.8362	0.0991	4.8350	-0.1415	6.7856	-0.0225	8.7321	0.2631
2.7150	-0.1525	3.8373	0.0665	4.8357	-0.1311	6.7860	-0.0416	8.7355	0.3452
2.7165	-0.1271	3.8380	0.0627	4.8364	-0.1195	6.7864	-0.0256	8.7362	0.3756
2.7176	-0.1595	3.8388	0.0564	4.8395	-0.1139	6.7871	-0.0310	8.7369	0.3776
2.7184	-0.1267	3.8399	0.0240	4.8402	-0.0901	6.7876	-0.0447	8.7379	0.4095
2.7192	-0.1242	3.8407	0.0160	4.8409	-0.1019	6.7880	-0.0428	8.7386	0.4159
2.7213	-0.1255	3.8414	0.0161	4.8419	-0.0982	6.7887	-0.0452	8.7393	0.4415
2.7221	-0.1198	3.8426	0.0045	4.8426	-0.0898	6.7891	-0.0332	8.7403	0.4495
2.7232	-0.1085	3.8434	-0.0086	4.8433	-0.0592	6.7895	-0.0514	8.7409	0.4838
2.7240	-0.1093	3.8442	-0.0352	4.8443	-0.0620	6.7902	-0.0554	8.7416	0.4481
2.7247	-0.1129	4.7291	0.0419	4.8450	-0.0454	6.7906	-0.0488	8.7428	0.4734
2.8191	-0.1356	4.7299	0.0503	4.8457	-0.0385	6.7910	-0.0494	8.7435	0.4906
2.8198	-0.1205	4.7307	0.0729	5.8200	0.4509	6.7935	-0.0792	8.7481	0.4750
2.8206	-0.1074	4.7319	0.0578	5.8208	0.4396	6.7942	-0.0689	8.7488	0.4542
2.8217	-0.1282	4.7326	0.0956	5.8217	0.4228	6.7949	-0.0869	8.7497	0.4597
2.8225	-0.1285	4.7333	0.0872	5.8228	0.3935	6.7968	-0.0888	8.7504	0.4299
2.8232	-0.1147	4.7357	0.1502	5.8237	0.3608	6.7978	-0.0902	8.7511	0.4361
2.8248	-0.1279	4.7367	0.1661	5.8245	0.3320	6.7985	-0.0878	8.7523	0.4134
2.8256	-0.1334	4.7374	0.1625	5.8256	0.3073	6.7992	-0.0919	8.7530	0.3762
2.8263	-0.1136	4.7381	0.1813	5.8265	0.2836	6.8024	-0.1130	8.7537	0.3638
2.8275	-0.1327	4.7637	0.3587	5.8273	0.2653	6.8031	-0.1161	8.7851	-0.1167
2.8282	-0.0953	4.7643	0.3445	5.8284	0.2420	6.8038	-0.0962	8.7858	-0.1438
2.8290	-0.0861	4.7650	0.3062	5.8292	0.2007	6.8048	-0.1116	8.7867	-0.1540
2.8343	-0.0829	4.7660	0.2832	5.8301	0.2015	6.8055	-0.1089	8.7874	-0.1553
2.8351	-0.0765	4.7667	0.2652	5.8341	0.1276	6.8062	-0.1244	8.7881	-0.1608
2.8359	-0.0451	4.7674	0.2578	5.8348	0.1085	6.8071	-0.1279	8.7891	-0.1702
2.8369	-0.0288	4.7684	0.2318	5.8355	0.0864	6.8078	-0.1213	8.7898	-0.1684
2.8377	-0.0475	4.7691	0.2212	5.8365	0.0651	6.8085	-0.1199	8.8442	0.1016
2.8384	-0.0465	4.7698	0.1840	5.8376	0.0427	6.8096	-0.1117	8.8449	0.1268
2.8395	-0.0596	4.7708	0.2029	5.8382	0.0403	6.8103	-0.1296	8.8456	0.1529
2.8403	-0.0169	4.7715	0.1564	5.8393	0.0494	6.8110	-0.1198	8.8465	0.1880
2.8410	-0.0050	4.7722	0.1448	5.8400	0.0291	6.8286	-0.0593	8.8472	0.2124
2.8421	-0.0339	4.7732	0.1286	5.8407	0.0037	6.8141	-0.1352	8.8479	0.2354
2.8429	0.0079	4.7739	0.1110	5.8445	-0.0357	6.8148	-0.1188	8.8483	0.2374
2.8437	-0.0193	4.7746	0.0982	5.8452	-0.0138	6.8155	-0.1208		
3.7169	0.1946	4.7755	0.0807	5.8459	-0.0199	6.8165	-0.1079		

TABLE 1
(Continued)

R OBSERVATIONS									
JD HEL. 2447830+	DELTA R MAG	JD HEL. 2447830+	DELTA R MAG	JD HEL. 2447830+	DELTA R MAG	JD HEL. 2447830+	DELTA R MAG	JD HEL. 2447830+	DELTA R MAG
2.6347	0.3917	3.7321	0.0257	4.7987	-0.0970	6.7454	0.5241	8.7027	-0.0698
2.6354	0.4130	3.7328	0.0274	4.7996	-0.1130	6.7461	0.5345	8.7063	-0.0245
2.6360	0.4317	3.7339	0.0133	4.8003	-0.1119	6.7468	0.5448	8.7070	-0.0228
2.6373	0.4400	3.7347	0.0161	4.8010	-0.1163	6.7478	0.5364	8.7077	-0.0162
2.6380	0.4575	3.7354	0.0125	4.8043	-0.1339	6.7485	0.5393	8.7089	-0.0160
2.6388	0.4717	3.7469	-0.0436	4.8050	-0.1219	6.7492	0.5298	8.7140	0.0196
2.6427	0.4770	3.7476	-0.0562	4.8057	-0.1355	6.7501	0.5369	8.7147	0.0415
2.6434	0.4723	3.7484	-0.0487	4.8069	-0.1374	6.7508	0.5466	8.7153	0.0311
2.6442	0.4776	3.7495	-0.0477	4.8076	-0.1239	6.7515	0.5403	8.7163	0.0622
2.6455	0.4605	3.7502	-0.0511	4.8083	-0.1316	6.7525	0.5412	8.7170	0.0598
2.6462	0.4518	3.7510	-0.0565	4.8093	-0.1319	6.7531	0.5424	8.7177	0.0613
2.6470	0.4641	3.7520	-0.0633	4.8100	-0.1402	6.7538	0.5408	8.7212	0.0944
2.6482	0.4266	3.7528	-0.0660	4.8107	-0.1350	6.7548	0.5363	8.7219	0.1177
2.6490	0.4108	3.7536	-0.0669	4.8116	-0.1404	6.7555	0.5484	8.7226	0.1355
2.6497	0.3913	3.7552	-0.0759	4.8123	-0.1254	6.7562	0.5337	8.7235	0.1326
2.6540	0.2969	3.7559	-0.0689	4.8130	-0.1323	6.7593	0.4702	8.7242	0.1222
2.6547	0.2858	3.7567	-0.0698	4.8162	-0.1202	6.7600	0.4425	8.7249	0.1471
2.6555	0.2673	3.7603	-0.0622	4.8169	-0.1390	6.7607	0.4191	8.7287	0.2296
2.6567	0.2400	3.7610	-0.0589	4.8176	-0.1244	6.7616	0.4064	8.7294	0.2305
2.6574	0.2233	3.7618	-0.0688	4.8186	-0.1191	6.7627	0.3771	8.7301	0.2584
2.6582	0.2109	3.8060	0.3654	4.8193	-0.1157	6.7634	0.3505	8.7311	0.2727
2.6593	0.1706	3.8068	0.3719	4.8200	-0.1104	6.7653	0.2912	8.7318	0.2774
2.6600	0.1649	3.8075	0.3863	4.8210	-0.1053	6.7662	0.2751	8.7325	0.2995
2.6608	0.1589	3.8088	0.4220	4.8217	-0.1112	6.7669	0.2613	8.7360	0.3448
2.6644	0.0767	3.8096	0.4314	4.8224	-0.1053	6.7676	0.2501	8.7367	0.3986
2.6651	0.0774	3.8103	0.4446	4.8234	-0.1129	6.7687	0.2250	8.7374	0.4024
2.6659	0.0500	3.8116	0.4582	4.8241	-0.1147	6.7694	0.2092	8.7383	0.4191
2.6669	0.0542	3.8123	0.4588	4.8248	-0.1036	6.7701	0.2032	8.7390	0.4365
2.6678	0.0337	3.8131	0.4717	4.8283	-0.1074	6.7736	0.1258	8.7397	0.4549
2.6686	0.0236	3.8142	0.4904	4.8290	-0.0933	6.7858	0.0099	8.7407	0.4498
2.6696	0.0199	3.8149	0.4798	4.8297	-0.0864	6.7862	0.0125	8.7414	0.4658
2.6703	0.0071	3.8157	0.4692	4.8306	-0.0857	6.7867	0.0163	8.7421	0.4828
2.6711	0.0054	3.8194	0.4613	4.8313	-0.0976	6.7874	-0.0092	8.7432	0.4688
2.6721	0.0006	3.8202	0.4436	4.8320	-0.0794	6.7878	0.0036	8.7439	0.4855
2.6728	-0.0200	3.8211	0.4377	4.8331	-0.0811	6.7882	0.0022	8.7446	0.4712
2.6736	-0.0233	3.8223	0.4218	4.8337	-0.0755	6.7889	-0.0031	8.7478	0.4619
2.6774	-0.0496	3.8232	0.4006	4.8344	-0.0703	6.7893	-0.0200	8.7485	0.4502
2.6782	-0.0516	3.8241	0.3751	4.8354	-0.0734	6.7897	-0.0098	8.7492	0.4318
2.6789	-0.0575	3.8254	0.3470	4.8361	-0.0624	6.7904	-0.0126	8.7501	0.4624
2.6801	-0.0706	3.8261	0.3183	4.8368	-0.0587	6.7908	-0.0131	8.7508	0.4647
2.6809	-0.0667	3.8269	0.3067	4.8400	-0.0409	6.7913	-0.0249	8.7515	0.4258
2.6816	-0.0770	3.8283	0.2695	4.8406	-0.0388	6.7939	-0.0239	8.7528	0.4135
2.6858	-0.0973	3.8291	0.2546	4.8413	-0.0566	6.7946	-0.0267	8.7535	0.3805
2.6866	-0.1037	3.8298	0.2526	4.8424	-0.0362	6.7953	-0.0322	8.7542	0.3643
2.6874	-0.1147	3.8351	0.1489	4.8431	-0.0189	6.7972	-0.0389	8.7585	0.2720
2.6886	-0.1195	3.8359	0.1294	4.8438	-0.0055	6.7982	-0.0477	8.7615	0.2074
2.6893	-0.1261	3.8366	0.1135	4.8448	-0.0068	6.7989	-0.0411	8.7682	0.0664
2.6901	-0.1391	3.8377	0.0940	4.8455	0.0069	6.7996	-0.0473	8.7689	0.0729
2.6912	-0.1168	3.8384	0.0739	4.8462	0.0345	6.8028	-0.0492	8.7696	0.0506
2.6920	-0.1221	3.8392	0.0677	5.8205	0.4641	6.8035	-0.0467	8.7706	0.0327
2.6927	-0.1362	3.8403	0.0533	5.8214	0.4383	6.8042	-0.0702	8.7848	-0.0728
2.6937	-0.1305	3.8411	0.0483	5.8222	0.4390	6.8052	-0.0676	8.7855	-0.0759
2.6945	-0.1374	3.8418	0.0435	5.8233	0.3978	6.8059	-0.0758	8.7862	-0.0836
2.6953	-0.1415	3.8430	0.0251	5.8242	0.3658	6.8066	-0.0627	8.7871	-0.1020
2.6963	-0.1480	3.8438	0.0223	5.8250	0.3488	6.8076	-0.0657	8.8043	-0.1461

TABLE 1
(Continued)

R OBSERVATIONS (Continued)									
JD HEL. 2447830+	DELTA R MAG	JD HEL. 2447830+	DELTA R MAG	JD HEL. 2447830+	DELTA R MAG	JD HEL. 2447830+	DELTA R MAG	JD HEL. 2447830+	DELTA R MAG
2.6971	-0.1479	3.8446	0.0060	5.8261	0.3144	6.8083	-0.0664	8.8047	-0.1355
2.6978	-0.1516	4.7296	0.0641	5.8270	0.2798	6.8089	-0.0752	8.8058	-0.1280
2.7082	-0.1379	4.7304	0.0790	5.8278	0.2758	6.8100	-0.0657	8.8062	-0.1437
2.7090	-0.1284	4.7312	0.0917	5.8289	0.2503	6.8107	-0.0722	8.8066	-0.1350
2.7097	-0.1361	4.7323	0.1047	5.8298	0.2314	6.8114	-0.0699	8.8073	-0.1245
2.7153	-0.0830	4.7330	0.1279	5.8306	0.2256	6.8145	-0.0740	8.8077	-0.1311
2.7169	-0.0830	4.7337	0.1250	5.8346	0.1393	6.8152	-0.0740	8.8081	-0.1264
2.7181	-0.0692	4.7347	0.0932	5.8353	0.1363	6.8159	-0.0678	8.8091	-0.1371
2.7188	-0.0723	4.7354	0.1212	5.8360	0.1238	6.8169	-0.0707	8.8098	-0.1323
2.7209	-0.0875	4.7361	0.1781	5.8369	0.1076	6.8176	-0.0755	8.8105	-0.1315
2.7217	-0.0734	4.7371	0.1803	5.8380	0.0908	6.8183	-0.0688	8.8136	-0.1121
2.7225	-0.0635	4.7378	0.2001	5.8387	0.0791	6.8194	-0.0676	8.8142	-0.1112
2.7236	-0.0626	4.7385	0.2019	5.8397	0.0791	6.8201	-0.0682	8.8149	-0.1001
2.7244	-0.0624	4.7641	0.3665	5.8404	0.0654	6.8208	-0.0623	8.8160	-0.1116
2.7251	-0.0531	4.7648	0.3358	5.8411	0.0660	6.8222	-0.0517	8.8167	-0.1077
2.8195	-0.0724	4.7655	0.3280	5.8449	0.0277	6.8229	-0.0512	8.8174	-0.1019
2.8202	-0.0748	4.7665	0.3045	5.8456	0.0171	6.8236	-0.0483	8.8184	-0.1181
2.8210	-0.0848	4.7672	0.2969	5.8463	0.0161	6.8281	-0.0324	8.8191	-0.1055
2.8221	-0.0905	4.7679	0.2698	5.8473	0.0121	6.8290	-0.0246	8.8198	-0.1010
2.8229	-0.0854	4.7689	0.2501	5.8480	0.0117	6.8297	-0.0230	8.8207	-0.0863
2.8236	-0.0542	4.7696	0.2573	5.8486	0.0133	6.8304	-0.0074	8.8214	-0.0900
2.8252	-0.0826	4.7703	0.2341	6.7007	-0.1205	6.8314	-0.0142	8.8221	-0.0624
2.8259	-0.0802	4.7712	0.1984	6.7014	-0.1225	6.8320	0.0006	8.8253	-0.0869
2.8267	-0.0733	4.7719	0.1760	6.7021	-0.1200	6.8327	0.0201	8.8260	-0.0682
2.8279	-0.0653	4.7726	0.1687	6.7031	-0.1155	6.8359	0.0428	8.8267	-0.0640
2.8286	-0.0705	4.7736	0.1521	6.7038	-0.1018	6.8366	0.0226	8.8277	-0.0667
2.8294	-0.0764	4.7743	0.1468	6.7044	-0.1123	6.8373	0.0470	8.8284	-0.0520
2.8347	-0.0702	4.7750	0.1303	6.7054	-0.1074	6.8382	0.0456	8.8290	-0.0393
2.8355	-0.0587	4.7760	0.1033	6.7061	-0.1086	6.8389	0.0470	8.8300	-0.0352
2.8373	-0.0533	4.7767	0.0949	6.7068	-0.0967	6.8396	0.0649	8.8307	-0.0356
2.8381	-0.0557	4.7773	0.0880	6.7078	-0.0914	6.8405	0.0560	8.8314	-0.0331
2.8399	-0.0443	4.7783	0.0636	6.7085	-0.0995	6.8412	0.0706	8.8324	-0.0246
2.8407	0.0256	4.7790	0.0563	6.7092	-0.0957	6.8419	0.0807	8.8371	0.0339
2.8414	-0.0050	4.7797	0.0392	6.7102	-0.0755	6.8430	0.0951	8.8378	0.0344
2.8425	-0.0180	4.7830	0.0073	6.7109	-0.0827	6.8436	0.0933	8.8385	0.0708
2.8433	0.0112	4.7836	0.0164	6.7116	-0.0838	6.8443	0.1151	8.8395	0.0723
2.8440	-0.0161	4.7843	0.0014	6.7158	-0.0506	6.8454	0.1261	8.8402	0.0799
3.7173	0.2310	4.7853	-0.0207	6.7165	-0.0522	6.8460	0.1316	8.8409	0.0976
3.7180	0.2120	4.7860	-0.0284	6.7172	-0.0381	8.6627	0.0255	8.8421	0.1226
3.7188	0.2145	4.7867	-0.0297	6.7181	-0.0282	8.6637	0.0152	8.8428	0.1390
3.7198	0.1824	4.7877	-0.0298	6.7188	-0.0251	8.6644	0.0184	8.8434	0.1648
3.7206	0.1672	4.7884	-0.0303	6.7195	-0.0311	8.6651	0.0272	8.8446	0.1761
3.7213	0.1508	4.7891	-0.0412	6.7205	-0.0225	8.6690	-0.0165	8.8453	0.2093
3.7225	0.1402	4.7901	-0.0450	6.7212	-0.0114	8.6696	-0.0278	8.8460	0.2336
3.7232	0.1171	4.7907	-0.0492	6.7218	-0.0006	8.6934	-0.0824	8.8469	0.2440
3.7240	0.1003	4.7914	-0.0594	6.7228	0.0057	8.6941	-0.0650	8.8476	0.2727
3.7250	0.0848	4.7925	-0.0626	6.7235	0.0238	8.6983	-0.0618	8.8483	0.2948
3.7257	0.0795	4.7932	-0.0745	6.7241	0.0316	8.6990	-0.0798		
3.7265	0.0767	4.7939	-0.0761	6.7432	0.4980	8.6997	-0.0678		
3.7302	0.0373	4.7973	-0.0897	6.7439	0.4931	8.7013	-0.0782		
3.7313	0.0264	4.7980	-0.1007	6.7446	0.5187	8.7020	-0.0870		

TABLE 1
(Continued)

I OBSERVATIONS									
JD HEL. 2447830+	DELTA IMAG	JD HEL. 2447830+	DELTA IMAG	JD HEL. 2447830+	DELTA IMAG	JD HEL. 2447830+	DELTA IMAG	JD HEL. 2447830+	DELTA IMAG
2.6349	0.3822	3.7330	-0.0019	4.7997	-0.1237	6.7463	0.5141	8.7014	-0.1080
2.6355	0.3970	3.7341	-0.0093	4.8004	-0.1144	6.7469	0.5053	8.7021	-0.0920
2.6362	0.4025	3.7348	-0.0039	4.8011	-0.1335	6.7479	0.4740	8.7028	-0.0869
2.6374	0.4320	3.7356	-0.0144	4.8044	-0.1300	6.7486	0.4898	8.7064	-0.0375
2.6382	0.4457	3.7470	-0.0770	4.8051	-0.1420	6.7493	0.4916	8.7071	-0.0280
2.6389	0.4322	3.7478	-0.0742	4.8058	-0.1542	6.7502	0.5007	8.7078	-0.0276
2.6428	0.4530	3.7485	-0.0815	4.8071	-0.1281	6.7509	0.5076	8.7090	-0.0097
2.6436	0.4487	3.7496	-0.0908	4.8077	-0.1431	6.7516	0.5043	8.7141	0.0010
2.6443	0.4229	3.7504	-0.0854	4.8084	-0.1406	6.7526	0.5149	8.7148	0.0173
2.6456	0.4410	3.7512	-0.0871	4.8094	-0.1443	6.7533	0.5060	8.7155	0.0149
2.6464	0.4403	3.7522	-0.0917	4.8101	-0.1518	6.7540	0.4961	8.7164	0.0306
2.6472	0.4238	3.7530	-0.0861	4.8108	-0.1631	6.7550	0.4739	8.7171	0.0575
2.6484	0.4033	3.7537	-0.0943	4.8117	-0.1434	6.7556	0.5044	8.7178	0.0416
2.6491	0.3834	3.7553	-0.1019	4.8124	-0.1562	6.7563	0.4816	8.7213	0.0825
2.6499	0.3596	3.7561	-0.0859	4.8131	-0.1543	6.7594	0.3999	8.7220	0.0799
2.6541	0.2852	3.7568	-0.1029	4.8163	-0.1389	6.7601	0.3957	8.7227	0.1087
2.6549	0.2596	3.7604	-0.0972	4.8170	-0.1577	6.7608	0.3691	8.7236	0.0757
2.6557	0.2418	3.7612	-0.0695	4.8177	-0.1467	6.7617	0.3644	8.7243	0.0989
2.6568	0.2148	3.7619	-0.0810	4.8188	-0.1254	6.7628	0.3545	8.7250	0.1026
2.6576	0.2105	3.8062	0.3423	4.8195	-0.1160	6.7635	0.3153	8.7288	0.2337
2.6584	0.1832	3.8069	0.3718	4.8201	-0.1123	6.7654	0.2453	8.7295	0.2246
2.6594	0.1592	3.8077	0.3884	4.8211	-0.1208	6.7664	0.2399	8.7302	0.2395
2.6602	0.1480	3.8090	0.4277	4.8218	-0.1239	6.7670	0.2146	8.7312	0.2617
2.6609	0.1477	3.8097	0.4458	4.8225	-0.1225	6.7677	0.1994	8.7319	0.2871
2.6645	0.0639	3.8105	0.4574	4.8235	-0.1508	6.7688	0.1768	8.7326	0.2879
2.6653	0.0430	3.8117	0.4584	4.8242	-0.1362	6.7695	0.1634	8.7361	0.3837
2.6660	0.0493	3.8125	0.4492	4.8249	-0.1674	6.7702	0.1554	8.7368	0.4138
2.6671	0.0320	3.8133	0.4660	4.8284	-0.1364	6.7737	0.0769	8.7375	0.4367
2.6679	0.0136	3.8143	0.4605	4.8291	-0.1211	6.7859	-0.0079	8.7384	0.4098
2.6687	0.0135	3.8151	0.4628	4.8298	-0.1321	6.7863	-0.0290	8.7391	0.4276
2.6697	-0.0039	3.8158	0.4439	4.8307	-0.1203	6.7867	-0.0126	8.7398	0.4309
2.6705	-0.0179	3.8195	0.4139	4.8314	-0.1071	6.7875	-0.0177	8.7408	0.4207
2.6713	-0.0214	3.8204	0.4150	4.8321	-0.0966	6.7879	-0.0039	8.7415	0.4372
2.6723	-0.0207	3.8213	0.4267	4.8332	-0.1076	6.7883	-0.0267	8.7422	0.4380
2.6730	-0.0409	3.8225	0.3987	4.8339	-0.0905	6.7890	-0.0064	8.7433	0.4328
2.6738	-0.0318	3.8234	0.3656	4.8346	-0.0833	6.7894	-0.0079	8.7440	0.4665
2.6776	-0.0634	3.8242	0.3302	4.8355	-0.0929	6.7898	-0.0388	8.7447	0.4488
2.6783	-0.0472	3.8255	0.3085	4.8362	-0.0884	6.7905	-0.0198	8.7479	0.4286
2.6791	-0.0518	3.8263	0.2969	4.8369	-0.0804	6.7909	-0.0354	8.7486	0.4140
2.6803	-0.0797	3.8271	0.2837	4.8401	-0.0461	6.7913	-0.0525	8.7493	0.4532
2.6810	-0.0880	3.8285	0.2307	4.8408	-0.0448	6.7940	-0.0434	8.7503	0.4376
2.6818	-0.0754	3.8293	0.2324	4.8415	-0.0557	6.7947	-0.0476	8.7510	0.4263
2.6860	-0.1094	3.8300	0.2275	4.8425	-0.0443	6.7954	-0.0488	8.7516	0.3854
2.6868	-0.1058	3.8353	0.1266	4.8432	-0.0193	6.7974	-0.0610	8.7529	0.3659
2.6875	-0.1320	3.8361	0.1140	4.8439	-0.0345	6.7983	-0.0684	8.7536	0.3531
2.6887	-0.1338	3.8368	0.0927	4.8449	-0.0186	6.7990	-0.0593	8.7542	0.3144
2.6895	-0.1327	3.8378	0.0807	4.8456	-0.0143	6.7997	-0.0665	8.7586	0.2321
2.6902	-0.1324	3.8386	0.0810	4.8463	0.0106	6.8029	-0.0853	8.7617	0.1576
2.6913	-0.1429	3.8394	0.0603	5.8207	0.4324	6.8036	-0.0893	8.7683	0.0528
2.6921	-0.1241	3.8405	0.0449	5.8215	0.4058	6.8043	-0.1023	8.7690	0.0626
2.6929	-0.1461	3.8412	0.0592	5.8223	0.4095	6.8053	-0.1089	8.7697	0.0345
2.6939	-0.1310	3.8420	0.0541	5.8235	0.3687	6.8060	-0.1026	8.7707	0.0115
2.6947	-0.1392	3.8432	0.0357	5.8243	0.3504	6.8067	-0.0995	8.7714	0.0375
2.6954	-0.1445	3.8440	0.0278	5.8252	0.3430	6.8077	-0.1001	8.7849	-0.0873
2.6964	-0.1518	3.8447	0.0076	5.8263	0.2690	6.8084	-0.1023	8.7856	-0.0858

TABLE 1
(Continued)

I OBSERVATIONS (Continued)									
JD HEL. 2447830+	DELTA IMAG	JD HEL. 2447830+	DELTA IMAG	JD HEL. 2447830+	DELTA IMAG	JD HEL. 2447830+	DELTA IMAG	JD HEL. 2447830+	DELTA IMAG
2.6972	-0.1601	4.7297	0.0653	5.8271	0.2872	6.8091	-0.0938	8.7863	-0.1026
2.6980	-0.1558	4.7306	0.0949	5.8279	0.2647	6.8101	-0.0983	8.7872	-0.1145
2.7084	-0.1495	4.7314	0.0899	5.8291	0.2440	6.8108	-0.0962	8.8044	-0.1388
2.7091	-0.1166	4.7325	0.1112	5.8299	0.2203	6.8115	-0.0868	8.8048	-0.1701
2.7155	-0.1192	4.7332	0.1289	5.8307	0.1783	6.8147	-0.0746	8.8059	-0.1354
2.7171	-0.1089	4.7339	0.1587	5.8347	0.1316	6.8154	-0.0799	8.8063	-0.1406
2.7182	-0.1041	4.7348	0.0600	5.8354	0.1203	6.8161	-0.0787	8.8067	-0.1507
2.7190	-0.0963	4.7355	0.1550	5.8361	0.0978	6.8170	-0.0733	8.8074	-0.1385
2.7211	-0.1033	4.7362	0.1762	5.8370	0.0697	6.8177	-0.0920	8.8078	-0.1361
2.7219	-0.0752	4.7372	0.1879	5.8381	0.0762	6.8184	-0.0776	8.8082	-0.1175
2.7226	-0.0662	4.7379	0.1847	5.8388	0.0734	6.8195	-0.0865	8.8092	-0.1448
2.7238	-0.0611	4.7386	0.2298	5.8398	0.0703	6.8202	-0.0748	8.8099	-0.1624
2.7245	-0.0798	4.7642	0.3388	5.8405	0.0545	6.8209	-0.0775	8.8106	-0.1306
2.7253	-0.0662	4.7649	0.3048	5.8412	0.0468	6.8223	-0.0563	8.8137	-0.1323
2.8196	-0.1182	4.7656	0.3123	5.8450	0.0200	6.8230	-0.0714	8.8144	-0.1349
2.8204	-0.1321	4.7666	0.2935	5.8457	0.0060	6.8237	-0.0565	8.8151	-0.1313
2.8212	-0.1218	4.7673	0.2596	5.8464	-0.0054	6.8282	-0.0392	8.8162	-0.1237
2.8223	-0.1250	4.7680	0.2577	5.8474	0.0033	6.8292	-0.0266	8.8168	-0.1301
2.8231	-0.1254	4.7690	0.2134	5.8481	0.0046	6.8298	-0.0259	8.8175	-0.1257
2.8238	-0.0934	4.7697	0.2111	5.8488	-0.0036	6.8305	-0.0340	8.8185	-0.1406
2.8254	-0.1414	4.7704	0.2141	6.7008	-0.1300	6.8315	-0.0234	8.8192	-0.1346
2.8261	-0.1017	4.7714	0.1735	6.7015	-0.1143	6.8321	-0.0220	8.8199	-0.1147
2.8269	-0.1156	4.7720	0.1590	6.7022	-0.1237	6.8328	-0.0208	8.8208	-0.1180
2.8280	-0.1066	4.7727	0.1703	6.7032	-0.1194	6.8360	-0.0155	8.8215	-0.0946
2.8288	-0.1079	4.7737	0.1470	6.7039	-0.1177	6.8367	0.0332	8.8222	-0.1065
2.8296	-0.1098	4.7744	0.1396	6.7045	-0.1263	6.8374	0.0210	8.8254	-0.1053
2.8349	-0.0775	4.7751	0.1205	6.7055	-0.1054	6.8383	0.0251	8.8261	-0.0858
2.8356	-0.0721	4.7761	0.0793	6.7062	-0.1130	6.8390	0.0157	8.8268	-0.0757
2.8375	-0.0835	4.7768	0.0739	6.7069	-0.1048	6.8397	0.0357	8.8278	-0.0657
2.8382	-0.0865	4.7775	0.0681	6.7080	-0.1126	6.8407	0.0319	8.8285	-0.0687
2.8401	-0.0601	4.7784	0.0546	6.7087	-0.1051	6.8414	0.0188	8.8292	-0.0510
2.8409	-0.0352	4.7791	0.0178	6.7094	-0.1172	6.8420	0.0363	8.8301	-0.0554
2.8416	0.0136	4.7798	0.0327	6.7103	-0.1138	6.8431	0.0553	8.8308	-0.0626
2.8427	-0.0335	4.7831	-0.0147	6.7110	-0.0943	6.8438	0.0789	8.8315	-0.0544
2.8435	-0.0163	4.7838	-0.0158	6.7117	-0.0923	6.8445	0.0633	8.8325	-0.0438
2.8442	-0.0279	4.7845	-0.0208	6.7159	-0.0462	6.8455	0.0868	8.8372	0.0190
3.7174	0.1939	4.7854	-0.0302	6.7166	-0.0568	6.8462	0.0999	8.8379	0.0146
3.7182	0.1704	4.7861	-0.0429	6.7173	-0.0569	8.6628	-0.0125	8.8386	0.0281
3.7190	0.1746	4.7868	-0.0410	6.7182	-0.0538	8.6638	-0.0132	8.8396	0.0323
3.7200	0.1331	4.7878	-0.0553	6.7189	-0.0283	8.6645	-0.0192	8.8403	0.0466
3.7208	0.1387	4.7885	-0.0450	6.7196	-0.0357	8.6652	-0.0050	8.8410	0.0558
3.7215	0.1277	4.7892	-0.0492	6.7206	-0.0210	8.6796	-0.0915	8.8422	0.0708
3.7226	0.1113	4.7902	-0.0675	6.7213	-0.0062	8.6803	-0.0763	8.8429	0.1155
3.7234	0.1027	4.7909	-0.0648	6.7220	0.0001	8.6851	-0.1098	8.8436	0.1416
3.7241	0.0796	4.7916	-0.0539	6.7229	0.0087	8.6865	-0.1143	8.8447	0.1391
3.7251	0.0529	4.7926	-0.0821	6.7236	0.0063	8.6902	-0.1120	8.8454	0.1658
3.7259	0.0395	4.7933	-0.0552	6.7242	0.0249	8.6909	-0.1345	8.8461	0.2042
3.7267	0.0424	4.7940	-0.0649	6.7433	0.4231	8.6935	-0.1118	8.8470	0.2251
3.7304	0.0039	4.7974	-0.0913	6.7440	0.4648	8.6985	-0.0922	8.8477	0.2636
3.7315	0.0029	4.7981	-0.1124	6.7447	0.4850	8.6992	-0.1011	8.8484	0.2742
3.7322	0.0005	4.7988	-0.1110	6.7456	0.5135	8.6999	-0.0965		

TABLE 2
Standard Magnitudes of YZ Phoenicis, Comparison and Check Stars

Star	V	B-V	V-R _C	R _C -I _C	V-I _C	Phase	Source
Comparison	12.776(8)	1.002(7)	0.609(7)	0.482(5)	1.093(7)	-	ST
Check	11.729(5)	0.674(28)	0.383(5)	0.354(8)	0.737(11)	-	ST
Variable	13.296(6)	0.953(14)	0.596(4)	0.518(4)	1.114(7)	0.00	ST
	12.675(14)	0.932(11)	0.571(4)	0.515(3)	1.087(2)	0.25	ST
	13.171(28)	0.949(13)	0.588(9)	0.513(7)	1.102(12)	0.50	ST
	12.580(5)	0.920(17)	0.553(6)	0.502(5)	1.057(6)	0.75	ST
	12.597(10)	0.882(5)	0.542(10)	-	1.028(13)	MAX	SJ
	13.257(15)	0.910(15)	0.577(8)	-	1.093(17)	MIN	SJ

Note: ST = Samec and Terrell (present paper), SJ = Jones (1989)

emerides with both their 0^d3052 period and the shorter period of KM. We find that the shorter period results in much smaller O-C residuals and gives initial ephemeris of

$$\text{JD (hel.) Min I} = 2436765^{\text{d}}.621(9) + 0.23472(7)E. \quad (1)$$

We note that this ephemeris has essentially the same period as calculated by KM for the present era! Thus, believing that the timings of GM were not at odds with those of the present era, we proceeded to fit all available timings by a single

linear least squares, weighting the photoelectric timings as 1.0 and all others as 0.1. We obtained

$$\text{JD (hel.) Min I} = 2445621^{\text{d}}.3976(9) + 0.23472693(8)E. \quad (2)$$

The O-C residuals calculated with ephemeris (2) are shown graphically in Fig. 1 and are listed as (O-C)₁ in Table 3. A second ephemeris was determined from photoelectric epochs, only:

TABLE 3
Epochs of Minimum Light, YZ Phoenicis

JD Hel. 2400000+	Minimum	Cycles	(O-C) ₁	(O-C) ₂	Source
36758.585	I	-37758.0	0.006954	0.011236	GM
36764.549	II	-37732.5	-0.014583	-0.010303	GM
36765.627	I	-37728.0	0.007146	0.011425	GM
36787.454	I	-37635.0	0.004541	0.008812	GM
36792.497	II	-37613.5	0.000912	0.005181	GM
36821.605	II	-37489.5	0.002772	0.007030	GM
36822.535	II	-37485.5	-0.006136	-0.001878	GM
45621.3968	I	0.0	-0.000757	0.000054	JO
47792.6220	I	9250.0	0.000282	0.000242	KM
47793.4425	II	9253.5	-0.000762	-0.000802	KM
47793.5610	I	9254.0	0.000374	0.000334	KM
47794.6160	II	9258.5	-0.000897	-0.000938	KM
47803.5355	II	9296.5	-0.001020	-0.001064	KM
47807.5260	II	9313.5	-0.000878	-0.000924	KM
47832.6428 (7)	II	9420.5	0.000090	0.000034	ST
47833.8166 (4)	II	9425.5	0.000282	0.000226	ST
47834.7557 (13)	II	9429.5	0.000507	0.000451	ST
47836.5165	I	9437.0	0.000845	0.000789	KM
47836.7515 (5)	I	9438.0	0.001108	0.001051	ST
47837.3370	II	9440.5	-0.000199	-0.000256	KM
47849.4265	I	9492.0	0.000864	0.000802	KM

Note: GM = Gessner & Meinunger (1975), JO = Jones (1989), KM = Kilkenny & Marang (1990), ST = Samec & Terrell (This paper)

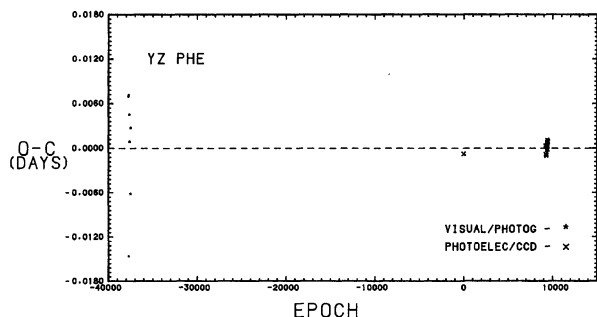


FIG. 1—Period behavior of YZ Phe indicated by all available data calculated from Eq. (2).

$$\text{JD (hel.) Min I} = 2445621^{\text{d}}3968(5) + 0.23472703(5)E. \quad (3)$$

This ephemeris was used to phase our observations and its residuals appear as $(O-C)_2$ in Table 3 and graphically in Fig. 2. Despite the large gap in the data, by scrutinizing Figs. 1 and 2 and by comparing Eqs. (1), (2), and (3) we conclude that the period of YZ Phe has not experienced a major period change in the course of 30 years. This is rather surprising since most previous studies of W UMa systems have revealed continuous period changes (both negative and positive) and/or abrupt period changes occurring with a frequency of 10 years or so (see discussion in Samec et al. 1993a). So this tentative result may be regarded with some suspicion. Period changes are thought to be linked with stellar magnetic cycles (Hall 1991) and angular momentum loss (AML) from stellar winds which should be prevalent in such a system (Guinan and Bradstreet 1988). To determine the true period behavior of this important system, observers should patrol it over the next decade or so and searches should be made of archived photographic plate collections.

5. LIGHT CURVES

The B , V , R , and I light curves of YZ Phe defined by the individual observations are plotted in Fig. 3 as Δm versus phase. The probable error for a single observation in B , V , R , and I is ± 0.009 , ± 0.008 , ± 0.006 , and ± 0.009 mag, respectively, so 1% photometry was realized. If more observations

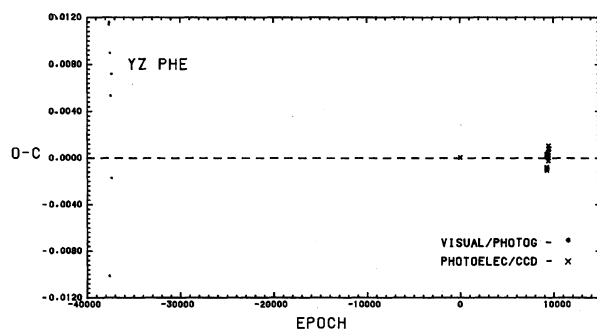


FIG. 2—O-C residuals of YZ Phe determined from Eq. (3) for photoelectric epochs of minimum light.

were taken, we believe that the errors would be somewhat larger due to night to night variations typically present in the light curves of VSP systems.

The light curves are typical of W UMa contact systems exhibiting a continual change in light output in the out-of-eclipse portion of the orbital cycle. A brief ~ 15 -min interval of constant light is discernible in the primary eclipse, particularly in the R and I light curves in Fig. 3. This indicates that YZ Phe is of W type with the primary, more-massive component being the cooler star.³ The $\Delta(B-V)$, and $\Delta(R-I)$ color curves are redder in the eclipses, and are reddest in the primary eclipses, due to gravity darkening on the backportions of the primary and secondary contact Roche lobes. A very significant O'Connell effect (Davidge and Milone 1984) is present in the light curves with Max II being 0.09, 0.08, 0.06, and 0.04 mag brighter than Max I in B , V , R and I , respectively. The asymmetry is very broad, affecting about 30% of the light curve. Conventional wisdom would indicate the existence of cool spots on the primary component on the side facing the observer near phase $0^{\text{p}}25$. The reason for this is that dynamo-driven magnetic fields arising from rapidly rotating convective atmospheres would likely induce them, especially on the primary, more deeply convective, component (Rucinski 1992). However, recent modeling of a similar system, CE Leo (Samec et al. 1993a), has shown that large regions with slightly elevated temperatures (i.e., faculae), may well represent this type of asymmetry. Multicolor photometry with close attention to the goodness-of-fit parameters is well suited to distinguish between these two alternatives. Further evidence could be gained from spectroscopic data taken with moderately sized telescopes and sensitive detectors. The hot spot should also be modeled on the primary component since it is most likely to have higher magnetic activity, but, in this case, would face the observer at phase $\sim 0^{\text{p}}75$, i.e., it would be $\sim 180^\circ$ out of orbital phase with the placement of a cool spot.

Specific characteristics of the ΔB , ΔV , ΔR , and ΔI light curves appear in Table 4. Magnitudes displayed in this table represent either averages over small intervals, typically $0^{\text{p}}02$ (i.e., the normal points), or those determined from a freehand curve carefully fitted to the observations.

6. PHOTOMETRIC SOLUTIONS

Synthetic light-curve solutions were calculated with the Wilson-Devinney (WD) Code (Wilson 1990, 1994; Wilson and Devinney 1971) which has a two-parameter bolometric limb darkening law for its detailed reflection treatment, and the ability to adjust spots with the differential corrections procedure. Here, we calculate the reflection effect to second order. In order to reduce the computational time on the Millikin University Microvax 3800, and to smooth out the scatter, 66 normal points, in units of intensity, were generated at each effective wavelength. Fixed bin widths of $0^{\text{p}}02$ in the out-of-eclipse portions of the light curve and $0^{\text{p}}01$ in the eclipse portions were used. As suggested in the 1992 "WD

³The common WD notation is that star 1 is the one occulted during the primary eclipse. Our 0.5 phase shift (see Sec. 6) has switched the star designations.

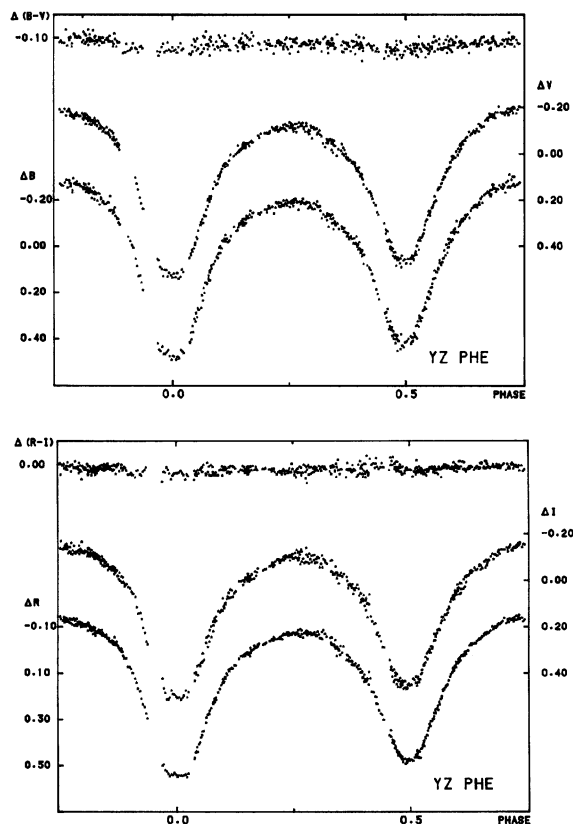


FIG. 3—*B*, *V*, *R*, and *I* light curves of YZ Phe as defined by the individual observations.

Documentation of Eclipsing Binary Computer Model,” normal points were weighted “intrinsically” according to the number of observations averaged. The *B*, *V*, *R*, *I* light curves were solved simultaneously in order to better fix temperature-related phenomena such as light values, spots,

and surface temperatures. Each curve was weighted in accordance with the standard deviation of a single observation in the light curves. The model-atmospheres option was used for atmosphere calculations. We chose the initial temperature of the primary component consistent with the system’s observed color indices. Linear limb-darkening coefficients, x_1 and x_2 , and bolometric limb-darkening coefficients, $xbol$, and $ybol$, were determined from tables by Van Hamme (1993). We chose the usual values of $A_1, A_2=0.5$, and $g_1, g_2=0.32$ for the bolometric albedoes and gravity darkening coefficients, respectively (Lucy 1967). The contact mode 3 of the dc program was used. To allow for phasing errors, Pshift (our ϕ), is used. We chose $\phi=0^{\circ}.5$ as a starting value, since the differential procedure runs faster when q is less than 1. Third light was not adjusted.

We started by assuming that the system had a dark spot on the cooler component, so we sought parameters which matched the curve everywhere, except at Max II. Consequently, before beginning the procedure, we removed the normal points in the area of the assumed (dark spot) asymmetry, from $\sim 0^{\circ}.09$ to $\sim 0^{\circ}.4$. From insight gained previously in the solving of similar light curves and by comparing our curves with those given in the Contact Binary Light Curve Atlas of Anderson and Shu (1979), we found a set of parameters needed to simulate the observed curves. Binary Maker 2.0 (Bradstreet 1992) was used throughout for initial curve fitting. Our set of starting parameters used in successfully initiating the dc procedure included $q=0.39$, inclination, $i=88^{\circ}$, $\Delta T=268$ K, and surface potential $\Omega=2.59$. A solution was obtained by simultaneously adjusting i, T_2, Ω, q , and L_1 . Next, the centroid of the spot was calculated and the width of the spot area was estimated from the O–C residuals of our solution. The spot-temperature factor ($T_{spot}/T_{photosphere}$) was varied along with additional changes in spot width until we attained what appeared to be a good fit to the observations. Next, we reinserted the formerly removed normal points and broke the large parameter setup into subsets, usually [$\{spot\ latitude, longitude\}, \{size, temperature\ factor\}$], [$\{\phi\}, \{i\}, \{T_2, \Omega\}, \{q, L\}$]. These were the only parameters adjusted in our solutions. The subsets were used to avoid the strong correlations between parameters. Each subset of parameters in the braces was allowed to adjust separately. Sometimes, particularly in later iterations, all these parameters were to adjust simultaneously when corrections were not unusually large. Many iterations were performed, and we found dc “dancing” around a very shallow local minimum. However, dc did converge to a dark-spot solution. It is given as model I in Table 5. The corresponding spot parameters are given in Table 6. The computed light curves are shown as Fig. 4. The synthetic light curves do not match our observations well around Max II. This was typical of all dark-spot calculations attempted (since we were new to this version of the program we tried various available options throughout our modeling work such as linear and nonlinear coefficients, the simplified versus the detailed reflection treatments, etc.). The model presented here is totally eclipsing. Early on, in the modeling procedure, we determined a solution which was not totally eclipsing ($i\sim 82^{\circ}$, and $q\sim 0.47$). However, it did not give a good fit to the eclipse portions of the light curve,

TABLE 4
Light-Curve Characteristics of YZ Phoenicis

Delta Mag at Minima and Maxima						
Phase	0.00 (MinI)	0.25 (MaxI)	0.50 (MinII)	0.75 (MaxII)		
ΔB	0.476	-0.195	0.427	-0.281		
ΔV	0.534	-0.113	0.473	-0.188		
ΔR	0.542	-0.071	0.476	-0.132		
ΔI	0.501	-0.105	0.450	-0.149		
$\Delta(B-V)$	-0.057	-0.081	-0.045	-0.093		
$\Delta(R-I)$	0.041	0.034	0.026	0.017		
Comparison of Minima						
		I	II	Diff.		
Depth (B) from Max. at Phase 0.25:		0.671	0.622	-0.049		
Depth (B) from Max. at Phase 0.75:		0.757	0.708	-0.049		
Average Depth (B):		0.714	0.665	-0.049		
Depth (V) from Max. at Phase 0.25:		0.647	0.586	-0.061		
Depth (V) from Max. at Phase 0.75:		0.722	0.661	-0.061		
Average Depth (V):		0.685	0.623	-0.061		
Depth (R) from Max. at Phase 0.25:		0.612	0.546	-0.066		
Depth (R) from Max. at Phase 0.75:		0.674	0.608	-0.066		
Average Depth (R):		0.643	0.577	-0.066		
Depth (I) from Max. at Phase 0.25:		0.611	0.560	-0.051		
Depth (I) from Max. at Phase 0.75:		0.674	0.608	-0.051		
Average Depth (I):		0.630	0.580	-0.051		
Comparison Between Maxima						
Filter	B	V	R	I	B-V	R-I
Difference (Max II - Max I)	-0.086	-0.075	-0.062	-0.044	-0.011	-0.018
Average of Maxima:	-0.238	-0.151	-0.101	-0.127	-0.087	0.025

TABLE 5
Synthetic Light-Curve Parameters for YZ Phoenicis

Parameter	Model I (Cool Spot)	Model II (Hot Spot)
λ_B (nm)	440	440
λ_V (nm)	550	550
λ_R (nm)	640	640
λ_I (nm)	790	790
$x_{1B} = x_{2B}$	0.898	0.898
$x_{1V} = x_{2V}$	0.755	0.755
$x_{1R} = x_{2R}$	0.651	0.651
$x_{1I} = x_{2I}$	0.545	0.545
$g_1 = g_2$	0.32	0.32
$A_1 = A_2$	0.50	0.50
$xbol_1 = xbol_2$	0.640	0.640
$ybol_1 = ybol_2$	0.153	0.153
i	$84^\circ.4$ (3)	$82^\circ.4$ (2)
T_1, T_2 (K)	$4800(100)^1, 5036(6)^2$	$4800(100)^1, 5055(7)^2$
$\Omega_1 = \Omega_2$	2.654 (5)	2.677 (4)
q	0.408 (3)	0.402 (2)
$L_1/(L_1+L_2)_B$	0.647 (3)	0.651 (3)
$L_1/(L_1+L_2)_V$	0.638 (3)	0.636 (4)
$L_1/(L_1+L_2)_R$	0.632 (3)	0.645 (4)
$L_1/(L_1+L_2)_I$	0.626 (4)	0.654 (4)
ϕ	0.4995 (7)	0.4993 (2)
l_3	0.00	0.00
r_1, r_2 (pole)	0.4387 (6), 0.2921 (22)	0.4336 (4), 0.2844 (14)
r_1, r_2 (side)	0.4698 (8), 0.3057 (27)	0.4629 (5), 0.2967 (17)
r_1, r_2 (back)	0.4996 (9), 0.3442 (49)	0.4902 (6), 0.3304 (29)
ρ_1, ρ_2 (g/cm ³)	2.32, 3.15	2.45, 3.45
fillout	16%	2%
Σwr^2	0.05417	0.03294

¹Photometric Uncertainty²Difference Uncertainty in $(T_2 - T_1)$

and had the same problems as the other dark-spot solutions.

Next, we moved the spot around $\sim 180^\circ$ in longitude and made the temperature factor $(T_{\text{spot}}/T_{\text{photosphere}}) > 1$ (higher than the surrounding atmosphere). The parameters converged rather emphatically to model II given in Table 5. The corresponding hot-spot parameters are included in Table 6. The computed light curves are shown as Fig. 5 and the geometric representation of YZ Phe at $0^{\text{h}}25^{\text{m}}$ with the spot is shown in Fig. 6, where the Roche lobe surface was produced by the MAC version of Binary Maker (Bradstreet 1992). Densities and fill outs in Table 5 were also calculated using Binary Maker. The Σwr^2 residual (the goodness of fit parameter) for the hot-spot solution is about half that for the dark-spot solution. Thus, our simultaneous computations show that the four-color photometry of YZ Phe, strongly favors the presence of a large radius superluminous region instead of a dark-spot region usually invoked to model asymmetries on convective contact binaries. This is the second system (Samec et al. 1993a) for which we have arrived at this rather emphatic result.

TABLE 6
Star Spot Parameters for YZ Phoenicis

Spot parameters	Model I (Cool spot)	Model II (Hot spot)
Location	Primary	Primary
Colatitude	66° (13)	94° (26)
Longitude	$88:7$ (9)	$257:6$ (22)
Spot radius	49° (4)	54° (4)
Temperature factor	0.964 (6)	1.031 (4)
Spot temperature (K)	4627 (29)	4945 (19)
Spot area	17 (2)	21 (2)
(% of total area of component)		

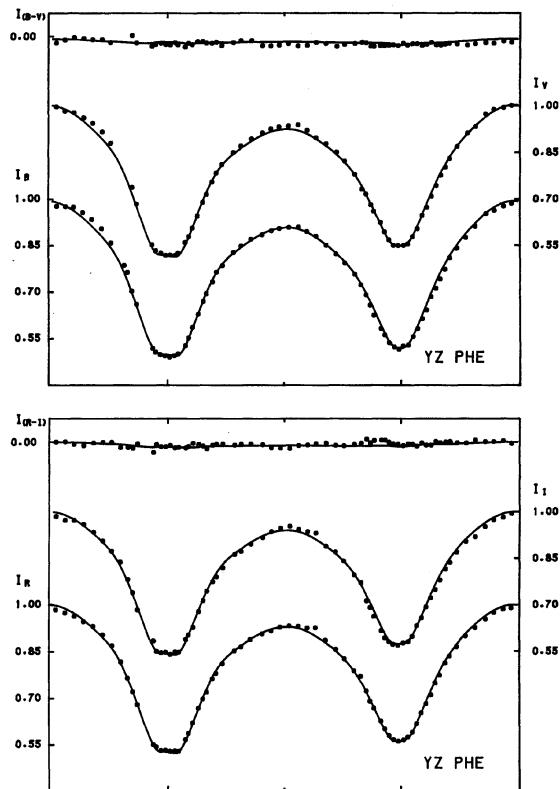


FIG. 4— B, V, R, I intensity light curves as defined by observations (normal points) and computed light curves (model I, with cool spot) for YZ Phe.

7. DISCUSSION

The photometry, in conjunction with our lowest residual, model II, solution for YZ Phe indicates that the system consists of a K3(V) primary and a K2(V) secondary component with a mass ratio of ~ 0.4 in a state of marginal contact, $f \sim 2\%$, and a temperature difference, $\Delta T = 255$ K. This fill out is somewhat low for W UMa W-type binaries, which usually fall in the 10%–20% range (the errors do not allow a fill out greater than 6%). This could indicate that YZ Phe has recently come into contact since (Guinan and Bradstreet 1988) there is a weak positive correlation between space velocity (i.e., kinematical age and fill out). Its mass ratio falls right in the middle of the normal range for F or later spectral type W UMa-type systems, i.e., $q = 0.2$ – 0.6 . Since, most theories of the evolution of contact binaries predict that q decreases with contact age, we might infer that this binary began contact with a mass ratio near its present value with precontact spectral types of $\sim G8(V)$ and $\sim M3(V)$. However, its location on the high end of the period–color plane does admit to some contact evolution. Vilhu (1981, 1982) shows that as contact systems evolve toward smaller q 's, they progress toward lower $B - V$'s and somewhat longer periods. The dark-spotted model does seem to give a more consistent picture in this regard, with its higher fill out. Whatever its precontact condition, the expectation is that it will eventually coalesce into an $\sim F4$ spectral-type FK Comae fast-rotating variable star.

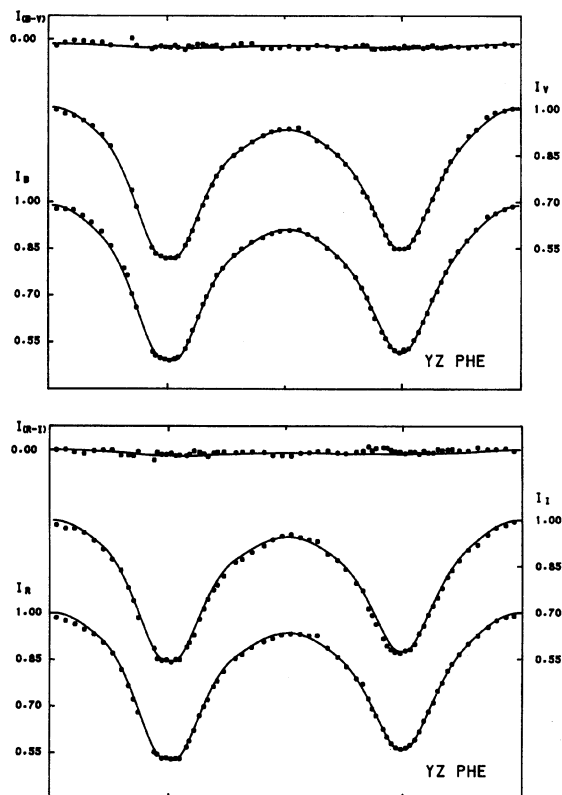


FIG. 5— B, V, R, I intensity light curves as defined by observations (normal points) and computed light curves (model II, with hot spot) for YZ Phe.

Rucinski (1992) has noted that the period distribution of contact systems has a well-defined short-period limit of $\sim 0^d.22$. Several explanations have been offered of this phenomenon. These include: the rapidity of orbital decay, poor statistics, and the attainment of the full convection, or Hayashi Limit as suggested by Rucinski (1992). Although our study of YZ Phe does not reveal a period change, several recently studied solar-type contact systems have continuous period decreases of 10^{-7} – 10^{-8} d/yr (Samec et al. 1993a). In addition to the systems mentioned in that paper, RW Com has a $\dot{P} = -1.5 \times 10^{-8}$ d/yr (Milone and Naftilan 1979). From this we could estimate the contact lifetime of these systems to be on the order 10^6 – 10^7 yr. However, if longer-period systems are undergoing AML, then they should provide a

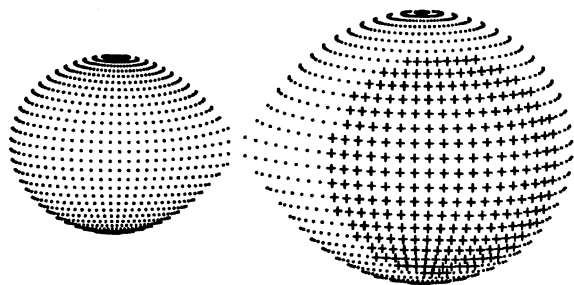


FIG. 6—Geometrical representation of YZ Phe at $0^p.75$ with superluminous area.

rather continuous source of VSP binaries in the future. So the orbital decay explanation is moot. Alternatively, one can argue that since the typical VSP system is faint, our statistical base is inadequate. Indeed, most known VSP systems lie in the 12^m – 15^m range. This is due to the late-spectral type of the dwarf stars making up the systems. And the very faintest ones are capable of having the shortest periods. We might predict that deep-sky CCD searches could reveal contact systems down to the dimensions of late M-type dwarfs. However, searches of this type have been made, in clusters. The results are that many contact or near-contact systems have been discovered in this manner but all have been found to have periods longer than the $0^d.22$ barrier. However, it can be argued that photometric errors of faint variables would hinder their discovery, especially for low-amplitude systems. Rucinski (1992) has made the interesting suggestion that sheds some light on this puzzle. Fully convective stars have a unique mass–radius relation that, in general, cannot be reconciled with that required by contact Roche lobe geometry. Thus, dynamically stable contact systems cannot exist with temperatures lower than this limit. For most configurations in VSP systems, the limit occurs at $B - V \sim 1.5$. This explains why contact systems with spectral types later than M1 (V) do not exist. However, there still remains a gap that is unexplained. The coolest VSP systems have color indices of ~ 1.25 [spectral types of $\sim K5$ (V)]. Where are the systems of intermediate temperatures, i.e., $1.5 > B - V > 1.25$? Rucinski states that some other physical process must be at play. YZ Phe, although it is one of the shortest-period systems observed, is far outside this limit with a $B - V \sim 0.9$. We must remember that the Roche Lobe approximation is just that, an approximation. Dense, near-fully convective dwarfs may no longer fulfill the assumptions of this approximation (Lai, Rasio, and Shapiro 1993): that is, a small condensed core overlaid by a highly compressible envelope and atmosphere.

A discussion of large hot-spot regions on more massive components of VSP systems is found in Samec et al. (1993a). Hot spots on contact systems may be explained as the result of matter in transit through the “neck” of the Roche lobes, etc. (Lu 1991). However, they may simply be due to the predominance of white-light faculae (Guinan 1990) on such systems. Doppler imaging (Piskunov and Rice 1993) of brighter contact binaries with large O’Connell effects may lend further support to the presence of hot spots on W UMa systems.

Further study of binaries near the short-period limit is certainly needed.

We wish to thank Marcelo de Arruda, an undergraduate student at Butler University, who did some preliminary analyses of this system which he presented at the 1992 Indiana Undergraduate Research Conference, Indianapolis, IN and Jamie D. Gray, now an undergraduate student at Millikin University, who performed many useful simulations both during and prior to the conference using the Binary Maker 2.0 software. He also aided in computing standard magnitudes and in setting up Table 1. Also, R.S. would like to thank his colleague, Brian Skiff of Lowell Observatory, for pointing out the problem in the SIMBAD data base.

REFERENCES

- Anderson, L., and Shu, F. H. 1979, *ApJS*, 40, 667
 Archer, S. 1959, *J. Brit. Astron. Assoc.* 69, 4, 157
 Bessell, M. S. 1976, *PASP*, 88, 557
 Bessell, M. S. 1979, *PASP*, 91, 589
 Bradstreet, D. H. 1992, *BAAS*, 24, 1125
 Davidge, T., and Milone, E. F. 1984, *ApJS*, 55, 571
 Dedoch, A. 1991, BRNO Contract No. 30, 49
 Eggleton, P. P. 1992, in *Evolutionary Processes in Interacting Binary Stars*, IAU Symposium No. 151 (Dordrecht, Kluwer), p. 167
 Gessner, H., and Meinunger, I. 1975, *I. VSS* 8 (5), 249 and 265
 Guinan, E. F. 1990, in *Proceedings of the International Symposium on Evolution in Astrophysics*, ESA SP-310, p. 73
 Guinan, E. F., and Bradstreet, D. H. 1988, in *NATO Advanced Study Institute on the Formation & Evolution of Low Mass Stars* (Dordrecht, Kluwer), p. 345
 Hall, D. S. 1991, *ApJ*, 380, L85
 Hardie, R. H. 1962, *Stars and Stellar Systems, Astronomical Techniques*, Vol. 2 (Chicago, University of Chicago Press), p. 18
 Henden, A. A., and Kaitchuck, R. H. 1990, *Astronomical Photometry* (Richmond, Willman-Bell)
 Hoffleit, D. 1963, *AJ*, 68, 207
 Hoffmeister, C. 1963, *VSS* 6(1), 53
 Holmgren, D. 1991, private communication
 Hut, P., et al. 1992, *PASP*, 681, 981
 Jones, S. 1989, *IBVS* No. 3296
 Kilkenny, D., and Marang, F. 1990, *IBVS* No. 3438
 Lai, D., Rasio, F. A., and Shapiro, S. L. 1993, *Cornell University Center for Radiophysics and Space Research Preprint No. 1019*
 Landolt, A. U. 1973, *AJ*, 78, 959
 Landolt, A. U. 1983, *AJ*, 88, 439
 Lu, W. 1991, *AJ*, 102, 262
 Lucy, L. B. 1967, *Zs. f. Ap.*, 65, 89
 Maceroni, C., Van Hamme, W., and Veer, van't 1990, *A&A*, 234, 177
 Milone, E. F., and Naftilan, S. A. 1979, in *Close Binary Stars: Observations and Interpretation* (Dordrecht, Reidel), p. 419
 Piskunov, N. E., and Rice, J. B. 1993, *PASP*, 105, 1415
 Popper, D. M. 1980, *ARAA*, 18, 115
 Rucinski, S. M. 1992, *AJ*, 103, 960
 Rucinski, S. M. 1993, in *The Realm of Interacting Binary Stars* (Dordrecht, Kluwer), p. 111
 Samec, R. G. 1989, *PASP*, 101, 661
 Samec, R. G. 1990, *AJ*, 100, 808
 Samec, R. G., and Bookmyer, B. B. 1987a, *PASP*, 99, 612
 Samec, R. G., and Bookmyer, B. B. 1987b, *PASP*, 99, 1310
 Samec, R. G., and Bookmyer, B. B. 1987c, *PASP*, 99, 1298
 Samec, R. G., Charlesworth, S. D., and DeWitt, J. R. 1991, *AJ*, 102, 688
 Samec, R. G., and Hube, D. P. 1991, *AJ*, 102, 1171
 Samec, R. G., Su, W., and DeWitt, J. R. 1993b, *PASP*, 105, 1441
 Samec, R. G., Su, W., Terrell, D., and Hube, D. P. 1993a, *AJ*, 106, 318
 Samec, R. G., Van Hamme, W., and Bookmyer, B. B. 1989, *AJ*, 98, 2287
 Soderblom, D. R., Stauffer, J. R., Hudon, J. D., and Jones, B. F. 1993, *ApJS*, 85, 315
 Tsuru, T., et al. *MNRAS*, 255, 192
 Van Hamme, W. 1993, *New Limb-Darkening Coefficients for Modeling Binary Star Light Curves*, preprint
 Vilhu, O. 1981, *Ap&SS*, 78, 401
 Vilhu, O. 1982, *A&Ap*, 109, 17
 Wilson, R. E. 1990, *ApJ*, 356, 613
 Wilson, R. E. 1994, *PASP*, 106, 921
 Wilson, R. E., and Devinney, E. J. 1971, *ApJ*, 166, 605